



Università degli Studi Mediterranea di Reggio Calabria
Archivio Istituzionale dei prodotti della ricerca

Asphalt Mixtures Modified With Basalt Fibers For Surface Courses

This is the peer reviewed version of the following article:

Original

Asphalt Mixtures Modified With Basalt Fibers For Surface Courses / Celauro, C; Pratico', Filippo Giammaria.
- In: CONSTRUCTION AND BUILDING MATERIALS. - ISSN 0950-0618. - 170:(2018), pp. 245-253.
[10.1016/j.conbuildmat.2018.03.058]

Availability:

This version is available at: <https://hdl.handle.net/20.500.12318/685> since: 2020-12-04T10:44:36Z

Published

DOI: <http://doi.org/10.1016/j.conbuildmat.2018.03.058>

The final published version is available online at: <https://www.sciencedirect>.

Terms of use:

The terms and conditions for the reuse of this version of the manuscript are specified in the publishing policy. For all terms of use and more information see the publisher's website

Publisher copyright

This item was downloaded from IRIS Università Mediterranea di Reggio Calabria (<https://iris.unirc.it/>) When citing, please refer to the published version.

(Article begins on next page)

ASPHALT MIXTURES MODIFIED WITH BASALT FIBRES FOR SURFACE COURSES

Authors

Celauro C. * & Praticò F.G.**

* Associate Professor, Department of Civil, Environmental, Aerospace, Materials Engineering (DICAM), University of Palermo. Italy.

E-mail: clara.celauro@unipa.it

** Associate Professor, DIIES Department, University Mediterranea of Reggio Calabria, Italy.

E-mail: filippo.pratico@unirc.it

Keywords: Asphalt mixture, Basalt fibres, Rutting resistance, Surface texture.

Abstract. *This paper shows the results of an experimental study concerning the effect of introduction of basalt fibres in asphalt mixtures for surface course, mainly with regard to those to be used in urban areas, for dedicated bus lanes. Surface layers, where tire-pavement interactions occur, have to provide different properties such as high friction (very important for users' safety), stability, resistance to meteorological agents, and contribution to the overall pavement performances. Considering that basalt fibres provide considerable physical and mechanical properties and above all high abrasion resistance, scope of the study is to evaluate the effects of these fibres on mixtures properties, especially in terms of friction and rutting behaviour.*

For this purpose, after setting up a model to estimate the impact of fibres on asphalt film thickness and richness modulus, the mixtures produced were subjected to laboratory tests for performance evaluation in terms of rutting resistance and the surface texture.

The test results allow drawing some important conclusions about basalt fibre-modified asphalt mixtures: in particular, these mixtures show better performance with reference to permanent deformation resistance when compared with the traditional mixture; moreover, the introduction of basalt fibres involves a "flattening" of the profile texture and a lower macrotexture. Interestingly, fibres addition is likely to slightly increase the micro-texture. This point calls for further study.

1 Introduction

The modern road pavements must meet many performance requirements in order to satisfy the current needs of the transport: not only due to the increasing traffic load that requires high mechanical performance; they must also ensure the movement of vehicles securely, smooth, safe and comfortable surfaces according to qualitative levels that depend on the category of road and the expected traffic.

Road safety is related to the quality of the surface layer of the pavement. In particular, adequate friction, in tire – road interaction, must be guaranteed in all situations, to allow the vehicle to maintain the chosen trajectory and efficient braking, especially in curve.

Another functional characteristic of the surface layers - the user's comfort - involves a series of factors related to surface characteristics of the road and in particular to the absence of irregularities, such as waves and degradations of any kind [1].

46 Nowadays, for sustainable development, research focuses on developing new technologies for
47 asphalt mixtures production in order to improve mechanical and functional performances and assure
48 the same performances specified by the current Technical Specification, also thanks to the use of
49 specific additives for achieving improved performances. Furthermore the use of specific additives
50 such as fibres or scrap materials is considered as an interesting and effective solution to face
51 environmental issues linked to reusing waste materials and to satisfy particular needs in road
52 technique [2].

53 At present, there are two research orientations to improve pavement performance of asphalt
54 mixture: one is to better asphalt non-deformability at high temperature, via improving aggregate
55 gradation, which is based on asphalt structure type and design procedures; the other is to better
56 asphalt mechanical performance and decrease temperature susceptibility, via improving asphalt
57 property and quality [3]. For the past few years, more and more new materials have been introduced
58 into the technology field of bituminous pavements. Thus, the third orientation to improve its
59 performance is formed, that is to add specific additives - fibres amongst these - to asphalt to
60 improve its physical and mechanical property.

61 At the moment, there mainly are three types of fibres applied in pavement project: cellulose fibres,
62 polyester fibres and mineral fibres [4]. Taking asphalt regeneration into consideration, mineral
63 fibres have been familiar to people, with better mechanical performance and higher work
64 temperature [5].

65 Basalt fibres (especially those obtained from scoria or vesicular basalt that cannot be directly used
66 as a construction material) can be considered environmentally friendly and non-hazardous
67 materials. It is not a new material, but its applications are surely innovative in many industrial and
68 economic fields, from building and construction to energy efficiency, from automotive to
69 aeronautic, thanks to its good mechanical, chemical and thermal performances. Hence, basalt fibre
70 has gained increasing attention as a reinforcing material especially if compared to traditional glass
71 fibres.

72 The production process, even if it is very similar to the glass fibres one, does not require additives
73 and a lower amount of energy is needed with benefits in terms of environmental impact, economics
74 and plants' maintenance. The base cost of basalt fibres depends on the quality and the chemical
75 composition of the raw material and this leads to have several kind of fibres with different thermal,
76 chemical and mechanical properties [6]. Indeed, the final cost of the fibres depends, at a large scale,
77 not only on the specific production process for the needed type of fibre, but also on the total
78 quantities to be produced. Many scientific studies confirm the growing interest on this type of fibres
79 [6-9].

80 There are so far few studies about the use of basalt fibres in the road pavement, all confirming their
81 good properties in terms of Marshall stability, rutting stability, water stability [5, 10, 11], the
82 possibility to have better low temperature performance, and the anti-fatigue property. Besides, at
83 high temperatures, the stiffness of asphalt mixture can be increased and permanent deformation can be
84 reduced [11, 12]. Thus, it is of interest to evaluate the benefit of introducing basalt fibres in surface
85 course for urban applications, in order to offer effective maintenance and rehabilitation options for
86 urban pavement management, as a valuable alternative to the use of polymer modified bituminous
87 mixtures.

88 **2 Objectives and main phases of the study**

89
90 The object of this research work is to evaluate the effect of the introduction of basalt fibres in
91 asphalt mixtures for surface courses, in terms of surface texture and permanent deformation
92 resistance, especially for use in urban areas, for dedicated bus lanes, where vertical stresses and
93 strain level are more severe [13], due to frequent stopping and restarting manoeuvres, both at bus
94 stops and at traffic lights [14].

95 The study is organized into the following main sections: modelling, design of experiments, material
 96 characterisation and mix design, results and discussions.
 97 A model to consider the impact of fibres on asphalt film thickness and richness modulus is set up.
 98 The consequent effect in determining the optimum binder content, as related to the binder film
 99 thickness, is then derived. The factorial plan of experiments is shortly summarized in the Design of
 100 experiments paragraph, while the Material characterization and mix design section fully provides
 101 the characterization of the materials used in this study. In the Results analysis and conclusions
 102 section key conclusions are drawn and main contributions are pointed out.

103 3. Modelling

104 In the pursuit of the above objectives, if analytical methods are used to estimate the specific surface
 105 area of aggregates [15], it is relevant to model the impact of fibres on two conceptually similar
 106 approaches to determine the optimum binder content: the asphalt film thickness (according to the
 107 Standard STP 204-19 [16]) and the richness modulus [17], fundamental to ensure mixture
 108 durability.

109 If the aggregates are modelled in terms of spheres (where D_A is the diameter, m) and the fibres are
 110 modelled in terms of cylinders (diameter: D_F , m, height L , m, $L/D_F \cong 800$), the specific surfaces,
 111 (SS_A , SS_F , respectively, m^2/kg), are approximated as follows:

$$112 \quad SS_A = \frac{6}{D_A \cdot G_{seA}} \quad (1)$$

$$113 \quad SS_F = \frac{4}{D_F \cdot G_{seF}} \quad (2)$$

114

115 where G_{se} refers to the effective specific gravity of aggregates/fibres.

116 Let the thickness (z , m) of the asphalt binder on the single particle be the function given by:

$$117 \quad z = \frac{\alpha^* \cdot D^{0.8}}{G_{se}^{0.2}} \quad (3)$$

118 It follows:

$$119 \quad z_A = \frac{\alpha_A^* \cdot D_A^{0.8}}{G_{seA}^{0.2}} = \frac{\alpha_A^*}{G_{seA}^{0.2}} \cdot \left(\frac{6}{SS_A} \right)^{0.8} \quad (4)$$

120 And

$$121 \quad z_F = \frac{\alpha_F^* \cdot D_F^{0.8}}{G_{seF}^{0.2}} = \frac{\alpha_F^*}{G_{seF}^{0.2}} \cdot \left(\frac{4}{SS_F} \right)^{0.8} \quad (5)$$

122 If K_D is the richness modulus of the bituminous mixture, as *per* Duriez formula [17], the
 123 percentages of bitumen (by weight of aggregates) are given by:

$$124 \quad b_A = \frac{\alpha_A^*}{G_{seA}} \cdot \left(\frac{6}{SS_A} \right)^{0.8} \cdot SS_A = \frac{\alpha_A^* \cdot 6^{0.8}}{G_{seD}} \cdot \frac{G_{seD}}{G_{seA}} \cdot SS_A^{0.2} = K_{DA} \cdot \alpha_A \cdot SS_F^{0.2} \quad (6)$$

$$125 \quad b_F = \frac{\alpha_F^*}{G_{seF}} \cdot \left(\frac{4}{SS_F} \right)^{0.8} \cdot SS_F = \frac{\alpha_F^* \cdot 6^{0.8}}{G_{seD}} \cdot \frac{G_{seD}}{G_{seF}} \cdot \left(\frac{4}{6} \right)^{0.8} \cdot SS_F^{0.2} = K_{DF} \cdot \alpha_F \cdot \beta_F \cdot SS_F^{0.2} \quad (7)$$

126 Where α is the well-known coefficient that takes into account the specific Gse, while β (which
127 pertains to the shape effects on the theoretical framework of Duriez and Arambide [17]) is herein
128 defined based on the equations above.

129 It turns out that if A% and F% are the percentages of aggregates and fibres (by total weight of non-
130 binder components) respectively (e.g., F=0.2%, A=99.8% [5, 10, 18]), the corresponding asphalt
131 binder percentage of the mixture (B, by total weight of aggregates/fibres) is the following:

$$132 \quad B = \frac{b_A \cdot A\% + b_F \cdot F\%}{A\% + F\%}. \quad (8)$$

133 In general terms, if $K_{DA}=K_{DF}=K_D$ (i.e., overall richness modulus according to Duriez), when the
134 traditional Duriez formula cannot be used due to very different shape characteristics of non-binder
135 components, the following algorithm is herein proposed:

$$136 \quad B = K_D \cdot \frac{\sum_i \alpha_i \cdot \beta_i \cdot SS_i^{0.2} b_i \cdot A_i \%}{\sum_i A_i \%} \quad (9)$$

137 Where each SS_i can be either expressed according to the given shape characteristics or in terms of
138 known correlations:

$$139 \quad SS_F = \frac{4}{G_{seF} \cdot D_F} \quad (10)$$

$$140 \quad 100 \cdot SS_A = 0.25 \cdot G + 2.3 \cdot S + 12 \cdot s + 135 \cdot f \quad (11)$$

141 where, G is the percentage of aggregate particles greater than 6.3mm, S between 0.25 and 6.3mm, s
142 between 0.075 and 0.25mm, f less than 0.075mm [19]:

143 Based on STP 204-19, the following algorithm applies in order to estimate the effective film
144 thickness (F_{be} , μm):

$$145 \quad F_{be} = \frac{981 \cdot P_{be}}{SST \cdot (100 - P_b)} \quad (12)$$

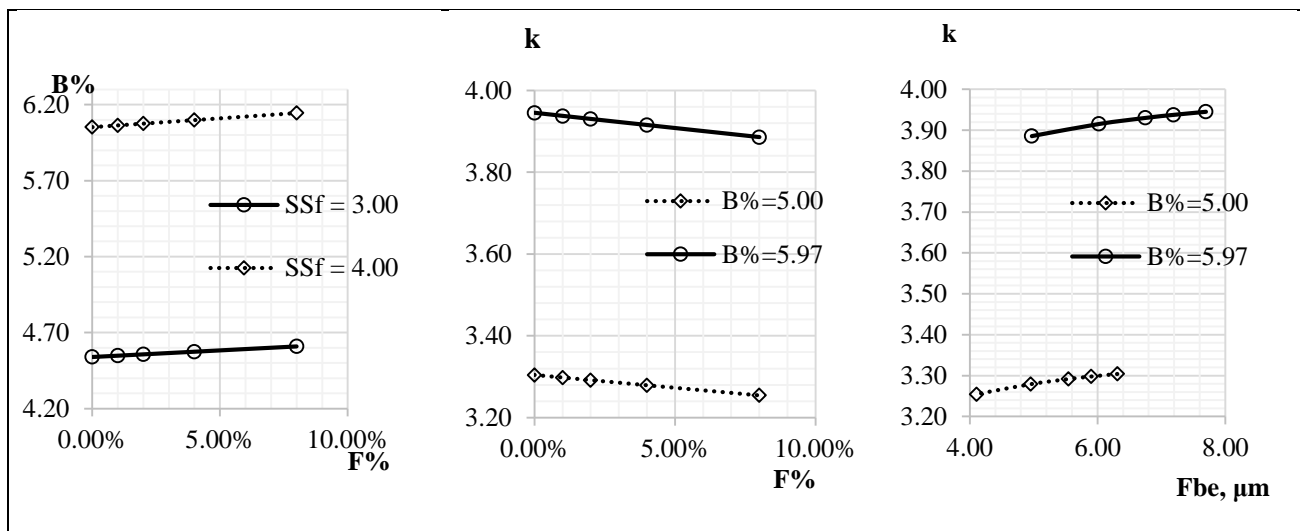
146 Where P_{be} (%) is the effective asphalt binder content by total mix weight (while B, %, is the asphalt
147 binder content by weight of aggregates), SST (m^2/kg) is the total surface area of the aggregate in the
148 mix, and P_b (%) is the (absorbed + effective) percent asphalt content by total mix basis. Note that:
149 i) the area factors specified in the concerned standard (STP 204-19) are different from the ones
150 specified in other standards and contexts (e.g., application of the Duriez formula [17] or Minnesota
151 Department of transportation adjusted asphalt film thickness [20]); ii) equations 1-10 are new, while
152 equations 11 and 12 derive from the literature. Based on the above, the relations among richness

153 modulus (k), binder percentage of the mixture ($B\%$), fibres percentage ($F\%$), and effective film
 154 thickness (F_{be}) are plotted in Figure 1.

155

156

157



158 *Figure 1. Relationships among bitumen content, richness modulus and effective film thickness*

159

160 It may be observed that: i) The higher the percentage of fibres is, the higher the bitumen percentage
 161 that is needed, for a given richness modulus (3 or 4); ii) The higher the percentage of fibres is, the
 162 lower the richness modulus becomes, for a given bitumen percentage (5.97% or 5.00%); iii) The
 163 higher the effective film thickness is, the higher the richness modulus is, for a given bitumen
 164 percentage (5.97% or 5.00%). Indeed, both k and F_{be} refer to the concept of bitumen coverage of
 165 grains (aggregate, fibres, etc.). Note from Figure 1 that when $F(\%) = 0$, for the selected range of
 166 SS_F , the corresponding values of k , $B\%$ and F_{be} above comply with the requirements given in
 167 literature for a durable mixture, i.e. a binder film thickness in the range of 6-8 μm [21, 22].

168 For B, the following supplementary requirements apply:

- 169
- 170 • B must comply with mechanistic/resistance requirements (e.g., resilient modulus, Marshall
Stability and quotient, etc.);
 - 171 • B must comply with volumetric requirements (e.g., air voids content, voids filled with
172 asphalt, voids of mineral aggregates);
 - 173 • B must comply with fatigue and rutting requirements;
 - 174 • B must comply with workability requirements. Indeed, the use of fibres may be useful to
175 improve the stiffness at higher temperatures and to reduce the stiffness at lower
176 temperatures. Unfortunately, along with several advantages, several construction-related
177 issues may emerge, which may include appropriate mixing and compaction temperatures
178 [23] and appropriate asphalt binder content. To this end, it is noted that in terms of
179 workability, mixtures with fibres usually require a slight increase on the optimum binder
180 content [24].
 - 181 • In case of friction courses, B must comply with functional requirements (e.g., surface
182 macrotexture, surface microtexture, and surface permeability/drainability, see [25]).

183 **4. Design of experiments**

184 Table 1 summarises the factorial plan of experiments. Three sets of tests were designed and carried
 185 out, namely case 1, case 2, and case 3.

186

187 *Table 1. Factorial plan of experiments*

	Case 1	Case 2	Case 3
Samples dimensions	305 x 305 x 50 mm		
Fibers percentage (F%)	0.0	0.0	0.3%
Aggregates percentage (A%)	100%	100%	99.7%
Bitumen	B 50/70	B 50/70	B 50/70
Richness modulus (K_D)	3.7	3.9	3.9
Tests and analyses	Material characterization (fibres, aggregates, asphalt binder) Marshall design/tests (SM , RM, vM) Rutting tests (RD) Surface texture (Z, LT, BPN, MPD, HS, AAD, AAH)		

Notes and symbols.
 SM: Marshall stability; RM: Marshall quotient; vM: Marshall air voids content; RD: ruth depth;
 z, LT, MPD, AAD, AAH: laser-based texture indicators (profile, texture level, mean profile depth, average
 asperity density, average asperity height); BPN: British pendulum number; HS: sand patch height.

188

189 **5. Material characterization and mix design**

190 **5.1 Material characterization (stone aggregates)**

191 The aggregates used in the mixtures are crushed limestone come from quarry whose
 192 composition and physical and mechanical properties are summarized in Table 2.

193

194

195 *Table 2. Physical and mechanical characteristics of the aggregates used.*

Characteristics	Fraction 15/20	Fraction 10/15	Fraction 5/10	Fraction 0/5	filler	Unit	Standard
Specific gravity (G_{se})				2.88	2.89	-	EN 1097-6 [26]
Apparent specific gravity (G_{sa})	2.83	2.84	2.86	2.87		-	EN 1097-6 [26]
Los Angeles abrasion (L.A.)	17.7	19.07	19.07			%	EN 1097-2 [27]
Micro Deval abrasion test in water (MDU)	8.5						ASTM D7428 – 15 [28]
Polished stone value (PSV)		0.40					EN 1097-8 [29]
Ridgen voids v					32,70	%	EN 1097-4 [30]
Sand equivalent (ES)				77		%	EN 933-8 [31]
Flakiness index (SI)	1.96	1.91					EN 933-3 [32]
Shape index (SI)	3.96	3.16				%	EN 933-4 [33]
Absorption coefficient	0.31	0.44	0.70	0.97			EN 1097-6 [26]

196

197 The available fractions as provided by the quarry were then combined according to the
 198 percentages given in Table 3, in order to comply with the typical limits [34] of a thin wearing
 199 course having layer thickness of about 3 cm (see Figure 2).

200

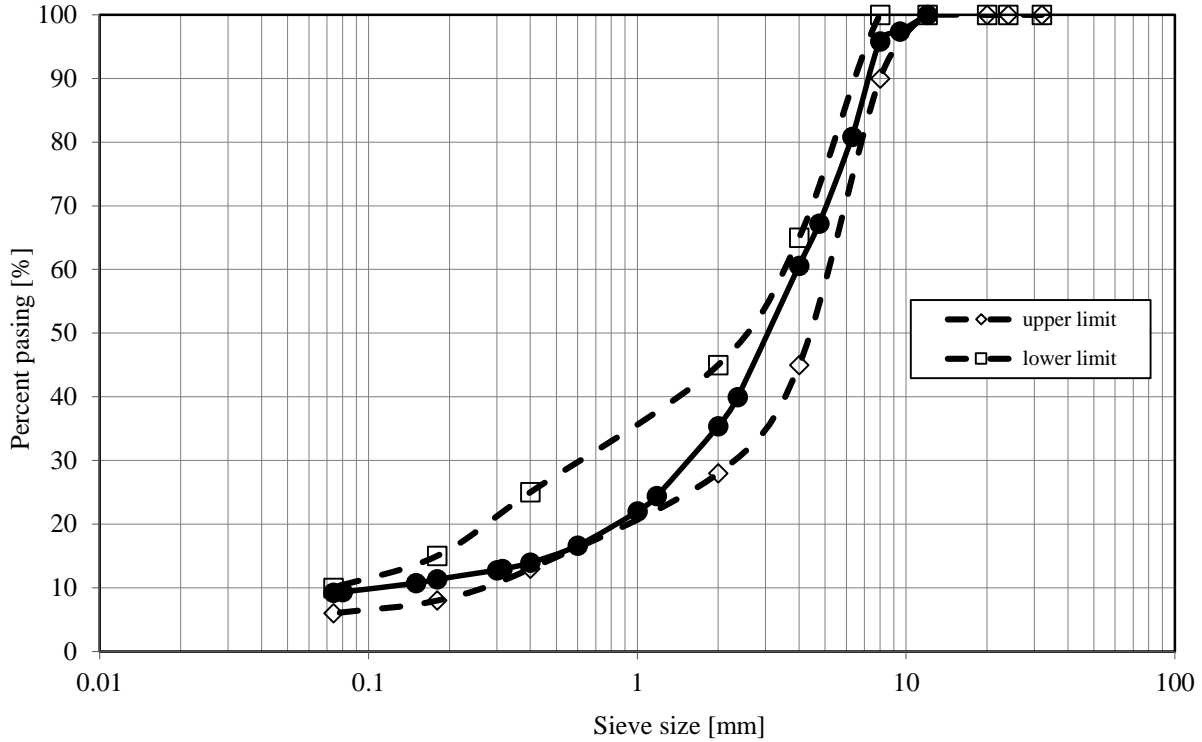
201

202

203 *Table 3. Percentage of each aggregate fraction combined for the target mixture*

	Fraction 15/20	Fraction 10/15	Fraction 5/10	Fraction 0/5	filler
(%)	0.48	0.20	0.14	0.17	1

204



205 *Figure 2. Mix grading curve.*

207

208 5.2 Material characterization (Bitumen)

209 The bitumen used is a pure bitumen, and due to its penetration it ranks between the hard
210 bitumen and semi-hard bitumen. Its characteristics are reported in Table 4.

211 *Table 4. Characteristics of the bitumen used in the studied mixtures.*

Characteristics	Unit	Values	Standard
Specific gravity at 25°C, γ	g/cm ³	1.033	ASTM D 70-76 [28]
Penetration at 25°C, pen	dmm	71	EN 1426 [35]
Softening point Ring and Ball, T _{R&B}	°C	47	EN 1427 [35]
Penetration Index, PI		-1.16	EN 12591 [36]
Colloidal Instability Index		0.17	
Viscosity at 135 °C	Pa·s	0.39	EN 13302 [37]
Viscosity at 160 °C	Pa·s	0.14	EN 13302 CEN [37]
After RTFOT:			
Penetration at 25°C, pen	Dmm	50	EN 1426 [38]
Softening point Ring and Ball, T _{R&B}	°C	51	EN 1427 [35]

213

214

215 The equiviscosity temperature is defined as the temperature corresponding to a viscosity of
216 the binder of $\eta = 170 \pm 20$ mPa·s. It refers to the mixing temperature of the bitumen with the

217 aggregate, during the production process. Measurements were carried out (Brookfield viscosity,
 218 AASHTO T 316 [39] and ASTM D 4402 [40]) over a range of different temperatures. The
 219 equiviscosity temperature found was $T_{eq} = 155 \text{ }^\circ\text{C}$ (case 1 and case 2). Note that equiviscosity
 220 does not take into account the effect on workability neither of aggregate shape and angularity on
 221 workability nor of fibres [23]. Studies carried out demonstrated that due to the presence of additives
 222 the equiviscosity may undergo an increase if fibres/modifiers are considered and asphalt binder
 223 content is not increased [41].

224 5.3 Material characterization (Fibres)

225 Basalt is a natural material that is found in volcanic rocks originated from frozen lava: it is a
 226 very common extrusion from many volcanic regions around the world. Basalt fibre is a material
 227 made from extremely fine fibres of basalt (basaltic rocks, including those with highly vesicular
 228 texture or scoria), melted under 1450-1500 $^\circ\text{C}$, and then processed into a continuous fibre.

229 Basalt fibres have a production cycle with lower energy impact than synthetic fibres, a high
 230 chemical stability, good resistance to weather, alkaline and acids exposure, low thermal
 231 conductivity, good mechanical properties, good thermal and acoustic insulation, high fire resistance,
 232 and an absolutely competitive cost compared to synthetic fibres [6].

233 Indeed, the good thermal stability of the basalt fibres is beneficial for insuring their stability in
 234 asphalt mixtures, during mixing, transportation and laying of the mixture itself. Furthermore, the
 235 basalt fibres are hydrophobic, thus limiting the water damage of the asphalt mixture [42].

236 Typically basalt fibres are produced in the form of chopped mat, roving and unidirectional
 237 fabric. In this study, they are cut into 3-5 millimetre pieces and their characteristics are given in
 238 Table 5. The introduction of these in the mixtures took place via dry method, after the aggregate:
 239 the fibres were added to the hot aggregates, before the bitumen. Normal mixing procedure, after
 240 visual inspection, proved to guarantee a good uniformity of the fibres into the mixtures. The
 241 selected fibres content was equal to 0.3% by weight of aggregate, which complies with the literature
 242 [11]. Considering the specific gravity of the aggregate skeleton (according to the percentages of
 243 each fraction detailed in Table 4) and that of the fibres, the figure above corresponds to the 0.26%
 244 in volume (by volume of aggregate).

245 *Table 5. Characteristics of the fibres used.*

Characteristics	Unit	Values	Standard
Colour		Grey	
Specific gravity of unsized filament	g/cm^3	2.67	
Moisture content of basaltic rock	%	0.1	
Melting point	$^\circ\text{C}$	1350	
Filament diameter range	μm	10÷19	ASTM D578 [43]
Elongation at break	%	2.8	ASTM D2256 [44]
Elastic modulus	GPa	84	
Continuous max temperature	$^\circ\text{C}$	250° to 550 $^\circ\text{C}$ 1200° fire barrier	
Moisture content	wt%	≤ 0.1	ISO 3344 [45]
Ignition loss		≥ 0.3	
Combustibility	M0	Pass	NFP 92-503 [46]
UV stability		6	ISO 105-B02 [47]
Colour fastness		6	ISO 105-X12 [48]

248 5.4 Preliminary mix design

249 Marshall Test was performed in order to carry out the preliminary mix design. Furthermore,
 250 this allowed complying with the physical and mechanical characteristics typically considered in
 251 Italian/European specifications (EN 12697-34). Two target richness moduli, K_D , were selected, as
 252 *per* Table 8.

253 The optimal percentage was found based on mix design, carried out according to the Marshall
 254 method, for the control mixture (case 1, see Table 9). Based on the given gradation (see Figure 2),
 255 the optimal bitumen percentage (by weight of aggregate) resulted between 5 and 6%.

256 The results, in terms of Marshall Stability, S_M , Marshall flow, f_M , Rigidity Ratio, R_M (Marshall
 257 quotient, ratio of stability to flow), and Marshall voids, v_M , for the optimal mixture, and the
 258 corresponding voids filled with bitumen, VFB, are given in Table 6.

259
 260 *Table 6. Marshall test results (case 1-reference)*

b [%]	S_M [kN]	f_M [mm]	R_M [KN/mm]	v_M [%]	VFB [%]
5.55	14.78	2.91	5.082	3.5	78.4

261
 262
 263 For comparison, typical requirements recommended for K_D , S_M , R_M , and v_M (commonly used
 264 French and Italian specifications) are given in Table 7.

265
 266 *Table 7. Marshall test requirements of Italian Specifications.*

Course	Autostrade per l'Italia S.p.A. [49]	MIT [34]	ANAS [50]	SNV [51]
Surface	$S_M > 11$ kN $R_M = 3 \div 4,5$ kN/mm $v_M = 4 \div 5$ %	$S_M > 11$ kN $R_M = 3 \div 4,5$ kN/mm $v_M = 3 \div 6$ %	$S_M > 10$ kN $R_M > 3$ kN/mm $v_M = 3 \div 6$ %	$K_D = 3.4-4.5$

267
 268 Note that, based on equations (9) to (12), the following results were obtained in terms of
 269 aggregates and fibres asphalt film and richness modulus (see Table 8).

270
 271 *Table 8. Average volumetric properties of the selected mixes*

	Case 1	Case 2	Case 3
Fibers percentage (F%)	0.0	0.0	0.3
Aggregates percentage (A%)	100	100	99.7
Bitumen, penetration grade	B 50/70	B 50/70	B 50/70
Richness modulus (K_D), design	3.7	3.9	3.9
Richness modulus (K_D), validation	3.67	3.94	3.95
B (by weight of aggregate, %)	5.55	5.97	5.97
Fbe, μm	7.10	7.52	7.70
DP (dust proportion)	1.77	1.69	1.64
Marshall air voids (%)	3.5	3.1	2.9
VFB (%)	78.4	80.3	82

272
 273 No relevant effect due to fibres introduction was noticed, as proved by the quite consistent
 274 Marshall air void results for the mixtures studied (case 2 and case 3 in Table 8).

275 6. Results and discussions

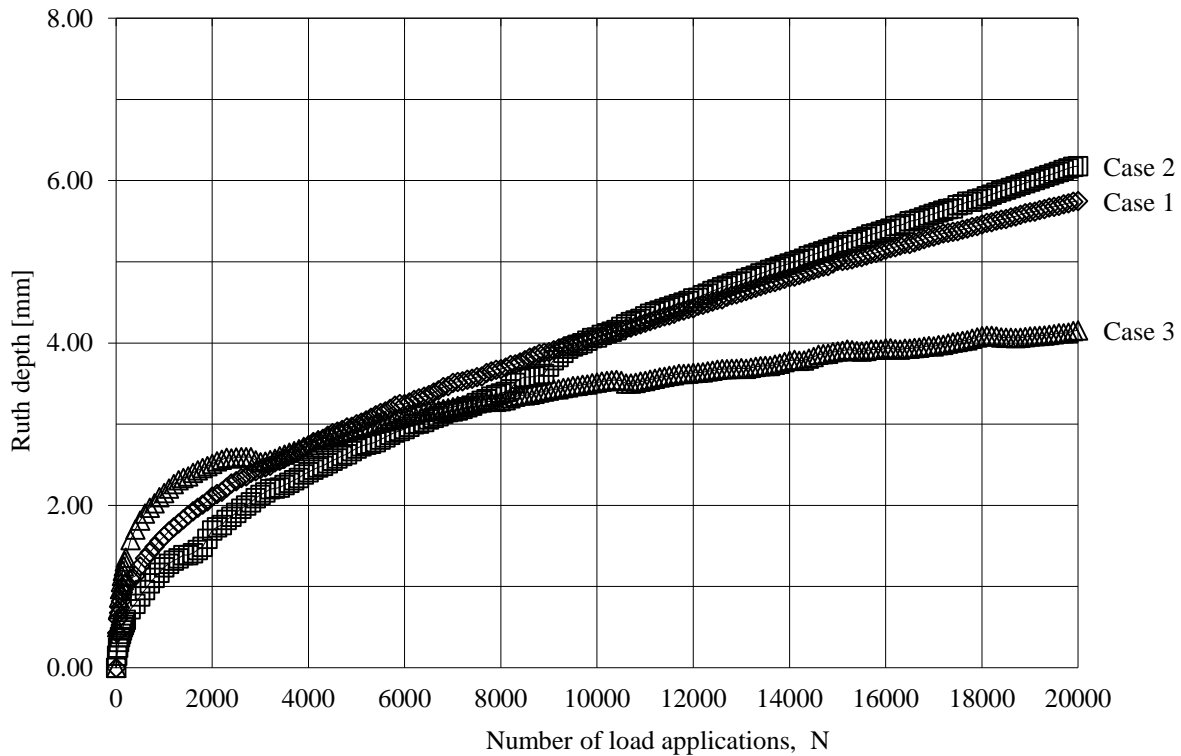
276 6.1 Permanent deformation resistance

277 In order to evaluate the permanent deformation resistance, the following mixtures were
 278 prepared: i) Mixtures with a binder dosage corresponding to the value $K_{D1} = 3.7$ (optimal dosage
 279 according to Marshall tests, case 1); ii) Fibre-added mixtures with a richness modulus of 3.9 (K_{D2})
 280 and a corresponding asphalt binder content of 5.97%; iii) Mixtures with a binder dosage
 281 corresponding to the value $K_{D3} = 3.9$, without fibres, for comparison purposes. It is noted that due
 282 to the slight percentage of fibres, the corresponding specific surface does not undergo a relevant

283 modification and consequently the richness modulus and the asphalt binder percentage of case 2 and
284 3 do not differ (rounding to tenths).

285 The wheel tracking test was carried out on slabs 305 x 305 x 50 mm in dimension, produced
286 per each mixture to be studied at fixed residual air voids set equal to the optimum Marshall for the
287 reference mixture ($v = 3.5\%$), according to EN 12697-22 standard (Method B). The average values
288 of rut depth are reported in Figure 3.

289



290

291 *Figure 3. Trend of rut depth in the wheel-tracking test.*

292

293 Note that: i) The higher the percentage of asphalt binder, the higher the rut depth after 10k-20k
294 passages, the higher (+18%) the first derivative (case 1 vs. case 2, no fibres); ii) The presence of
295 fibres implies lower rut depths after 10k-20k passages (-31%); iii) For the cases under investigation,
296 fibres imply lower rut depths for a given richness modulus (cases 2 and 3) and lower rut depths,
297 with respect to mixes with lower richness moduli, and lower asphalt film thicknesses (cases 3 and
298 1); iv) The addition of fibres implies an appreciable reduction of the first derivative (-53%). This
299 effect prevails over the effects due to film thickness/richness modulus.

300 The considerations above suggest a potential for lanes dedicated to urban public transit [14].

301

302 6.2 Surface texture

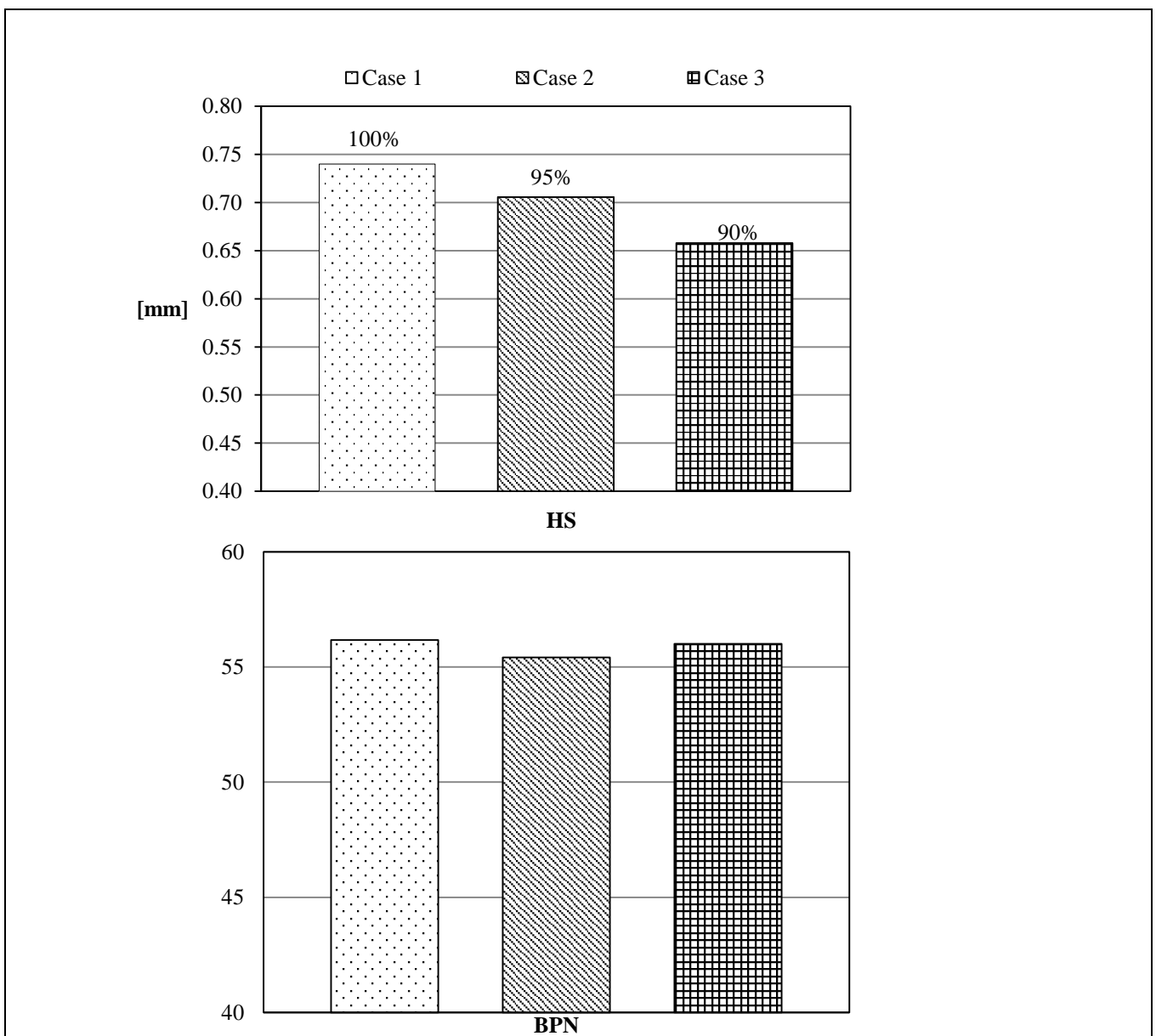
303 The surface texture of a pavement refers to its deviations from a planar and smooth surface. It
304 depends on a number of variables among which the nominal size of aggregate used and material
305 application rates. It affects skid resistance, rolling noise, and smoothness.

306 The links between cause "texture" and "effects" generated are represented by "indicators" of the
307 road surface, and these can be extrinsic or intrinsic. Among the indicators, there are HS (or MTD,
308 measured through the sand patch test, which pertains to macrotexture, ASTM E 965:1996) and BPN
309 (or PVT, slip/skid resistance of a surface, pendulum test, EN 13036-4:2011). Other indicators can
310 be derived based on the analysis of profiles $z(x)$ of the road surface (ISO 13473-2:2002), obtained

311 by instruments such as the “profilometers” [1]. This allows deriving mean profile depth (MPD, ISO
312 13473-1), texture level ($L_{tx, \lambda}$, ISO/TS 13473-4), average asperity density (AAD), and average
313 asperity height (AAH).

314 In this study, the following indicators were derived: HS, BPN, $L_{tx, \lambda}$, AAD, AAH, MPD. The
315 micro and macrot texture were evaluated by subjecting specimens to tests in order to determine the
316 surface characteristics because texture ranges influence the grip and thus the safety. As in previous
317 study, texture measurements were carried out on slabs produced in the laboratory using a lab-size
318 steel roller compactor [25]. This compaction method, that uses a roll segment to compact the loose
319 mix, is proved to be the most realistic in terms of arrangement of the aggregate, and thus it is
320 appropriate for producing samples to be tested for both functional and mechanical performances
321 [25, 52].

322 Sand patch test (macrot texture, [53]) was carried out according to ASTM E 965:1996 and the
323 average results in terms of sand height, SH, are given in Figure 4.
324



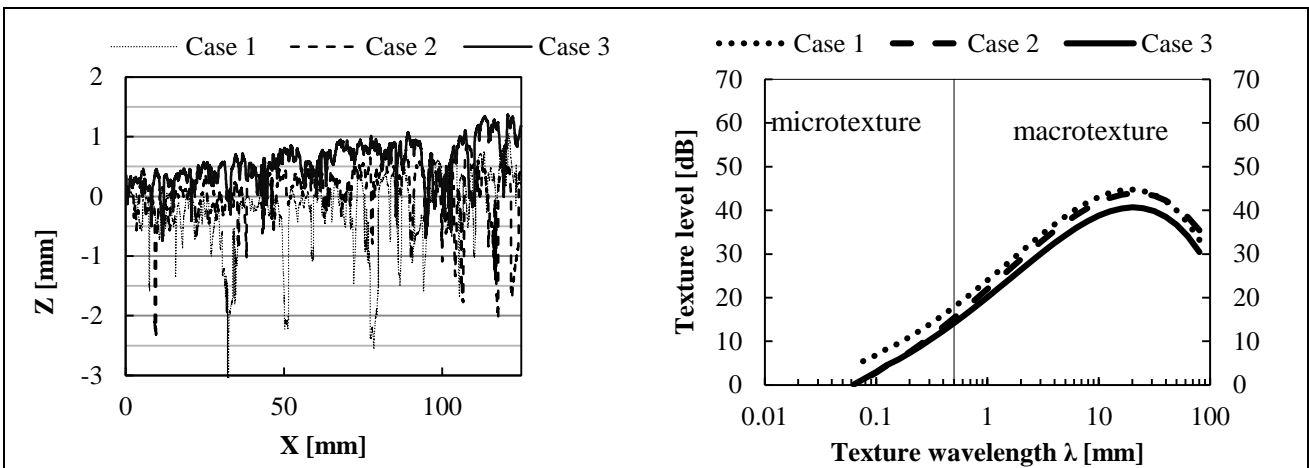
325 *Figure 4. Sand patch test results (HS) (top) and BPN values (bottom).*

326

327 It is possible to note that HS decreases when increasing bitumen content and adding fibres (fibres
 328 are a thickening agent); anyway these values comply with the minimum value required for the type
 329 of road (0.4 mm for urban and local streets).

330 Micro-texture values (BPN, Figure 4) are indirectly estimated in terms of pendulum test value,
 331 using low speed friction measurement devices such as the British Portable Tester British Pendulum
 332 Number (BPN) [53, 54]. Values appear to comply with Italian requirements for urban roads [34].
 333 Due to test repeatability, to the dependence on aggregates/fibres, the low percentage of fibres, the
 334 effects of fibre/bitumen are not evident.

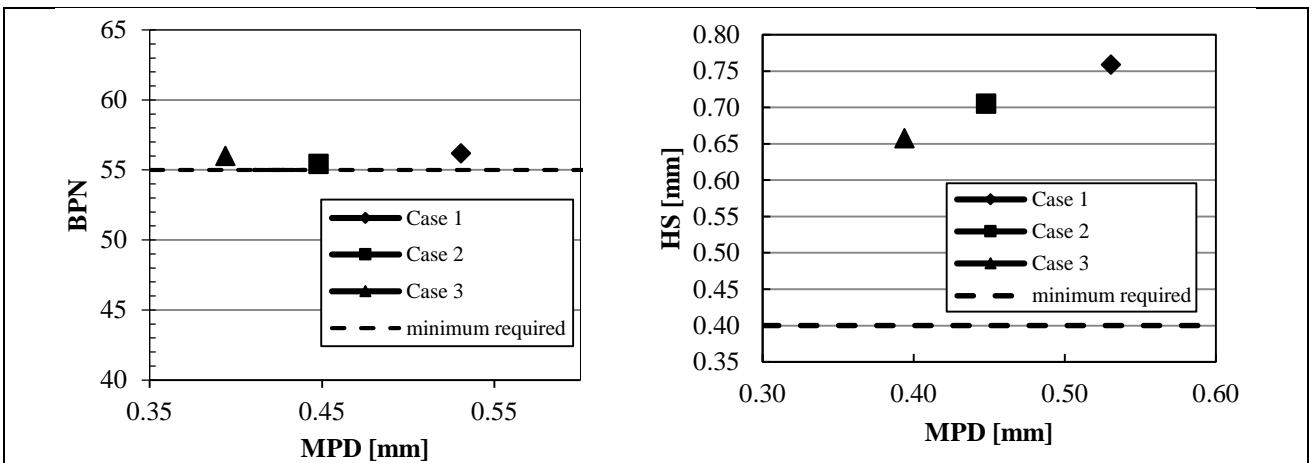
335 Additionally, a laser profilometer according to ISO/TS 13473-4 standard was used in order to
 336 obtain a characterization of the texture by direct measurements (ISO 13473-2:2002). This allowed
 337 deriving average profiles and texture level (Figure 5).
 338



339 *Figure 5. Profiles obtained (left) and texture spectra (right).*

340 In Figure 5 (right), the texture profile level, $L_{tx,\lambda}$, is represented (texture level: y-axis;
 341 wavelengths: x-axis, mm). Texture level builds on the logarithmic transformation of an amplitude
 342 representation of the profile curves $z(x)$ on the left. These latter are spectrally treated in terms root
 343 mean squares. It can be noted (Figure 5, left and right) that when increasing the bitumen content
 344 (cases 2 and 3) there is a smoothing of the surface and this is more evident in the mixture with the
 345 fibres (case 3).

347 When comparing BPN and MPD (Mean Profile Depth), as reported in Figure 6, it is possible to
 348 see that while MPD values change, BPN values are more or less the same for the mixtures studied.
 349

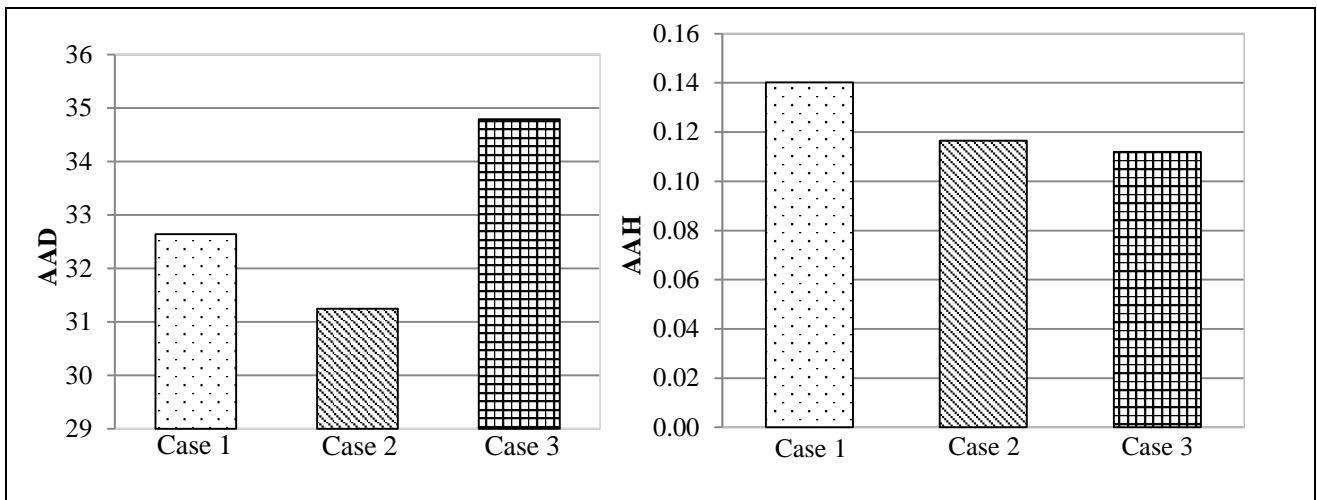


350 *Figure 6. Comparison between BPN and MPD (left) and between HS and MPD (right).*

351

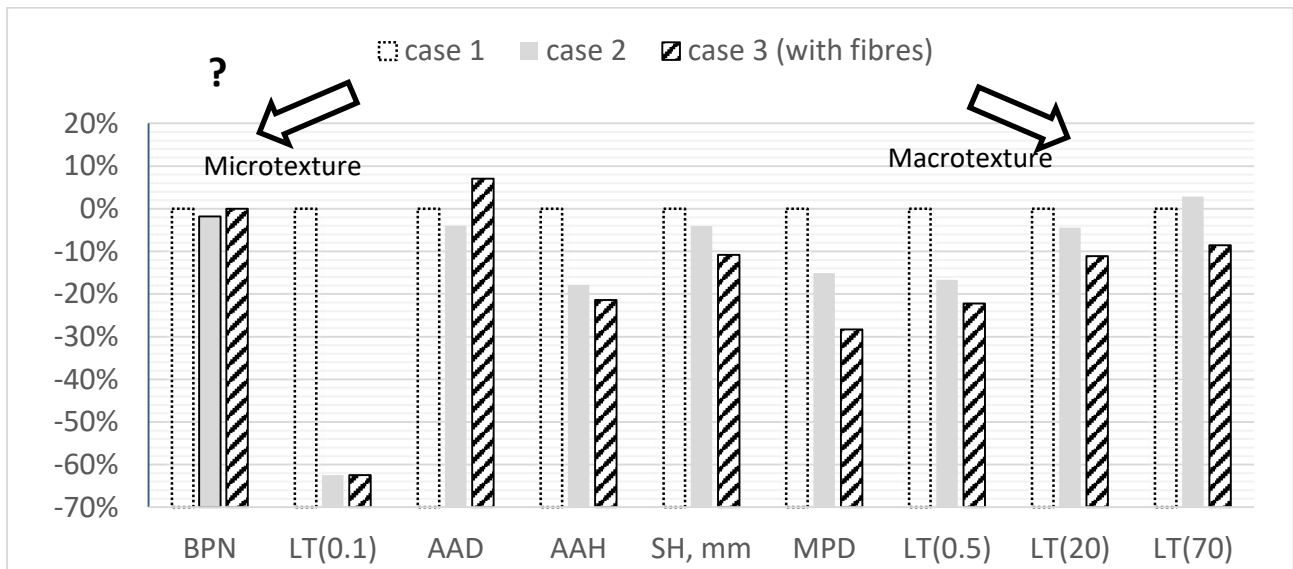
352 On the other hand, when comparing HS and MPD, as can be seen (Figure 6b), it can be noted
 353 that the mixture with the lowest richness modulus provides the highest macrotexture, while the
 354 mixture with basalt fibres (and higher richness modulus) provides a lower macrotexture (a sort of
 355 flattening of the surface tested). These conclusions are in line with the results of the indicators AAD
 356 and AAH for the different mixtures studied, depicted in Figure 7.

357 In any case, all the mixtures prove to provide values that comply with the minimum
 358 requirements for use as wearing course, so that it is possible to conclude that all the mixture studied
 359 offer adequate friction and resistance to the inevitable wear and tear, once in service.
 360



361 *Figure 7. Average asperity density (AAD) and average asperity height (AAH)*

362
 363



364 *Figure 8. Surface texture as a consequence of bitumen increase (case 2) and fibre addition (case 3)*
 365

366 In conclusion, based on the above, the following binary interpretation is proposed. For
 367 macrotexture ($\lambda > 0.5\text{mm}$, Cf. indicators on the right in Figure 8), the increase of bitumen content
 368 usually implies the smoothing of the texture profile and this is more marked in the mixture with
 369 basalt fibres where their presence tends to fill the macro-asperities. This last effect is even more
 370 evident in terms of texture spectrum ($L_{0.5}$ to L_{70}).
 371

372 For micro-texture ($\lambda < 0.5\text{mm}$, Cf. indicators on the left in Figure 8), the observations above
 373 seem not to apply: mixes 2 and 3, whose richness modulus is quite comparable, differ based on

374 fibre content. This latter is likely to slightly increase the micro-texture. This point calls for further
375 study as well as for the pertaining durability of texture-related effects. Indeed, there are the
376 technological uncertainties and limits because the diameter of the laser spot interacts with the
377 observable/ed wavelengths for the class of texture investigated [54].

378 **5 Conclusions**

379 The aim of this research was primarily to evaluate the effect of the introduction of basalt fibres
380 in asphalt mixtures for surface courses especially for use in urban areas, for dedicated bus lanes,
381 where vertical stresses and strain level are severer. Consequently, permanent deformation resistance
382 and surface texture were primarily investigated. In the pursuit of better controlling the factors (one-
383 factor-at-a-time), the problem was preliminary modelled and a specific algorithm was set up. Based
384 on results, the following conclusions can be drawn:

- 385 • in terms of rutting resistance, the introduction of basalt fibres proves to be beneficial;
- 386 • with regard to surface texture, the mixtures studied prove to fulfil both BPN (skid resistance,
387 microtexture) and HS (macrotexture) requirements for surface courses in urban contexts,
388 thus ensuring the required level safety for functional purposes;
- 389 • the macrotexture decreases when increasing the bitumen content and adding basalt fibres.
390 The same conclusions can be obtained by using the profilometers. In fact, when increasing
391 the bitumen content and through the introduction of basalt fibres, a smoothing effect on the
392 surface characteristics (asperities seem to be filled) is noted (texture spectra);
- 393 • importantly, the micro-texture seems to undergo a slight-to-negligible increase. BPN values
394 are more or less identical for the mixtures studied and this appears reasonable because this
395 parameter is mainly related to the characteristics of aggregates and the fibre content is quite
396 negligible. This notwithstanding, other microtexture-related indicators seem to appreciably
397 benefit from fibres. This point as well the durability/evolution over time of texture spectra
398 and properties call for future investigation.

399 Therefore, introduction of basalt fibres from vesicular basalt or scoria may be considered an
400 environmental-friendly and economical material for improving asphalt performance, in surface
401 course for urban applications, in substitution of commercial polymers.

402 **References**

- 403 [1] F. Praticò, R. Vaiana, A study on volumetric versus surface properties of wearing courses,
404 *Construction and Building Materials* 38 (2013) 766-775.
- 405 [2] C. Celauro, C. Bernardo, B. Gabriele, Production of innovative, recycled and high-performance
406 asphalt for road pavements, *Resources, Conservation and Recycling* 54(6) (2010) 337-347.
- 407 [3] M. Ranieri, L. Costa, J.R. M. Oliveira, H.M. RD Silva, C. Celauro, Asphalt Surface Mixtures
408 with Improved Performance Using Waste Polymers via Dry and Wet Processes, *Journal of*
409 *Materials in Civil Engineering* 29(10) (2017) 04017169.
- 410 [4] T.R. Board, E. National Academies of Sciences, Medicine, *Fiber Additives in Asphalt Mixtures*,
411 The National Academies Press, Washington, DC, 2015.
- 412 [5] N. Morova, Investigation of usability of basalt fibers in hot mix asphalt concrete, *Construction*
413 *and Building Materials* 47(Supplement C) (2013) 175-180.
- 414 [6] V. Fiore, T. Scalici, G. Di Bella, A. Valenza, A review on basalt fibre and its composites,
415 *Composites Part B: Engineering* 74(Supplement C) (2015) 74-94.
- 416 [7] V. Fiore, G. Di Bella, A. Valenza, Glass-basalt/epoxy hybrid composites for marine
417 applications, *Materials & Design* 32(4) (2011) 2091-2099.
- 418 [8] V. Fiore, F. Alagna, G. Di Bella, A. Valenza, On the mechanical behavior of BFRP to aluminum
419 AA6086 mixed joints, *Composites Part B: Engineering* 48(Supplement C) (2013) 79-87.

420 [9] G. Campione, L. La Mendola, A. Monaco, A. Valenza, V. Fiore, Behavior in compression of
421 concrete cylinders externally wrapped with basalt fibers, *Composites Part B: Engineering* 69 (2015)
422 576-586.

423 [10] Y.C. Cai, Y.X. Zheng, Experiment Study of Water Stability of Fiber-Reinforced Asphalt
424 Mixture, *Advanced Materials Research, Trans Tech Publ*, 2011, pp. 710-716.

425 [11] Y. Zheng, Y. Cai, G. Zhang, H. Fang, Fatigue property of basalt fiber-modified asphalt mixture
426 under complicated environment, *Journal of Wuhan University of Technology-Mater. Sci. Ed.* 29(5)
427 (2014) 996-1004.

428 [12] Y.X. Zheng, Y.C. Cai, Y.M. Zhang, Laboratory Study of Pavement Performance of Basalt
429 Fiber-Modified Asphalt Mixture, *Advanced Materials Research, Trans Tech Publ*, 2011, pp. 175-
430 179.

431 [13] D. Simard, F. Olard, Long-Life Overlays by Use of Highly Modified Bituminous Mixtures, in:
432 A. Scarpas, N. Kringos, I. Al-Qadi, L. A (Eds.), 7th RILEM International Conference on Cracking
433 in Pavements: Mechanisms, Modeling, Testing, Detection and Prevention Case Histories, Springer
434 Netherlands, Dordrecht, 2012, pp. 837-848.

435 [14] E.Y. Hajj, D. Batioja-Alvarez, R. Siddharthan, Assessment of Pavement Damage from Bus
436 Rapid Transit: Case Study for Nevada, *Transportation Research Record: Journal of the*
437 *Transportation Research Board* (2591) (2016) 70-79.

438 [15] R.P. Panda, S.S. Das, P.K. Sahoo, An empirical method for estimating surface area
439 of aggregates in hot mix asphalt, *Journal of Traffic and Transportation Engineering (English*
440 *Edition)* 3(2) (2016) 127-136.

441 [16] STP, STP 204-19 Asphalt film thickness determination, Standard test procedures manual,
442 Government of Saskatchewan Regina, Canada 2001.

443 [17] M. Duriez, J. Arrambide, *Nouveau traité de matériaux de construction: Liants et bétons*
444 *hydrocarbonés*, 2e édition ed., Dunod, Paris, 1962.

445 [18] S. Wu, Q. Ye, N. Li, H. Yue, Effects of fibers on the dynamic properties of asphalt mixtures,
446 *Journal of Wuhan University of Technology-Mater. Sci. Ed.* 22(4) (2007) 733-736.

447 [19] LCPC, Manuel LPC d'aide à la formulation des enrobés, Groupe de Travail RST "Formulation
448 des enrobés". Laboratoire Central des Ponts et Chaussées LCPC. Paris, France (2007).

449 [20] MnDOT, Adjusted Asphalt Film Thickness (AFT) in: M.D.o. Transportation (Ed.) MnDot, St.
450 Paul, MN 2017.

451 [21] B. Coree, W. Hislop, The difficult nature of minimum VMA: A historical perspective,
452 Presented to the Annual meeting, Transportation Research Board, Washington, DC (1999).

453 [22] W. Campen, J. Smith, L. Erickson, L. Mertz, The relationships between voids, surface area,
454 film thickness and stability in bituminous paving mixtures, *Proceedings, AAPT*, 1959.

455 [23] J. Gudimettla, J. L. Cooley, E. Brown, Workability of Hot-Mix Asphalt, *Transportation*
456 *Research Record: Journal of the Transportation Research Board* 1891 (2004) 229-237.

457 [24] A. Mahrez, M.R. Karim, RUTTING CHARACTERISTICS OF BITUMINOUS MIXES
458 REINFORCED WITH GLASS FIBER, *Journal of the Eastern Asia Society for Transportation*
459 *Studies* 7 (2007) 2168-2178.

460 [25] F.G. Praticò, R. Vaiana, T. Iuele, Macrotexture modeling and experimental validation for
461 pavement surface treatments, *Construction and Building Materials* 95 (2015) 658-666.

462 [26] CEN, EN 1097-6 Tests for mechanical and physical properties of aggregates-Part 6:
463 determination of particle density and water absorption, Comité Européen de Normalisation
464 Brussels, 2000.

465 [27] CEN, EN 1097-2. Tests for mechanical and physical properties of aggregates. Determination of
466 loose bulk density and voids, Comité Européen de Normalisation, Brussels, 1998.

467 [28] ASTM, D 70-76. Softening point, American Society for Testing Materials, West
468 Conshohocken, PA., 1976.

469 [29] CEN, EN 1097-8 Tests for mechanical and physical properties of aggregates. Determination of
470 the polished stone value, Comité Européen de Normalisation, Brussels, 2009.

471 [30] CEN, EN 1097-4 tests for mechanical and physical properties of aggregates: part 4—
472 determination of the voids of dry compacted filler, Comité Européen de Normalisation Brussels,
473 1999.

474 [31] CEN, EN 933-8. Tests for geometrical properties of aggregates. Assessment of fines. Sand
475 equivalent test, Comité Européen de Normalisation, Brussels, 1997.

476 [32] CEN, EN 933-3 Test for geometrical properties of aggregates. Part 3: Determination of particle
477 shape. Flakiness index, Comité Européen de Normalisation, Brussels, 1997.

478 [33] CEN, EN 933-4. Tests for geometrical properties of aggregates. Determination of particle
479 shape. Shape index, Comité Européen de Normalisation, Brussels, 2008.

480 [34] MIT, Norme Tecnica di Tipo Prestazionale per Capitolati Speciali d'Appalto - Performance
481 based requirement for Technical Specifications for road works, Ministero delle Infrastrutture e dei
482 Trasporti, 2001.

483 [35] CEN, EN 1427. Bitumen and bituminous binders - Determination of the softening point - Ring
484 and Ball method, Comité Européen de Normalisation, Brussels, 2007.

485 [36] CEN, EN 12591 Bitumen and bituminous binders. Specifications for paving grade bitumens,
486 Comité Européen de Normalisation, Brussels, 2009.

487 [37] CEN, EN 13302 Bitumen and bituminous binders. Determination of dynamic viscosity of
488 bituminous binder using a rotating spindle apparatus, Comité Européen de Normalisation, Brussels,
489 2010.

490 [38] CEN, EN 1426. Methods of tests for petroleum and its products. Bitumen and bituminous
491 binders. Determination of needle penetration, Comité Européen de Normalisation, Brussels, 2000.

492 [39] AASHTO, T 316 Viscosity Determination of Asphalt Binder Using Rotational Viscometer.”
493 AASHTO Standards, American Association of State Highway and Transportation Officials,
494 Washington, DC, 2004.

495 [40] ASTM, ASTM D4402 / D4402M Standard Test Method for Viscosity Determination of
496 Asphalt at Elevated Temperatures Using a Rotational Viscometer, American Society for Testing
497 Materials, West Conshohocken, PA, 2015.

498 [41] Y. Yildirim, M. Solaimanian, T.W. Kennedy, Mixing and compaction temperatures for hot mix
499 asphalt concrete, Work 1250 (2000) 5.

500 [42] X. Gu, T. Xu, F. Ni, Rheological behavior of basalt fiber reinforced asphalt mastic, Journal of
501 Wuhan University of Technology-Mater. Sci. Ed. 29(5) (2014) 950-955.

502 [43] ASTM, ASTM D578 / D578M - 05 Standard Specification for Glass Fiber Strands, American
503 Society for Testing Materials, West Conshohocken, PA, 2011.

504 [44] ASTM, ASTM D2256 Standard Test Method for Tensile Properties of Yarns by the Single-
505 Strand Method, American Society for Testing Materials, West Conshohocken, PA, 1997.

506 [45] E. ISO, ISO 3344 Reinforcement products -- Determination of moisture content, International
507 Organization for Standardization, Geneva, Switzerland, 1997.

508 [46] AFNOR, NF P92-503 Sécurité contre l'incendie - Bâtiment - Essais de réaction au feu des
509 matériaux - Essai au brûleur électrique applicable au matériaux souples., Association Française de
510 Normalisation, Paris, 1995

511 [47] ISO, ISO 105-B02 Textiles -- Tests for colour fastness -- Part B02: Colour fastness to artificial
512 light: Xenon arc fading lamp test, International Organization for Standardization, Geneva,
513 Switzerland, 2013.

514 [48] ISO, ISO 105-X12 Textiles -- Tests for colour fastness -- Part X12: Colour fastness to rubbing,
515 International Organization for Standardization, Geneva, Switzerland, 2016.

516 [49] p.l.I. Autostrade SpA, Capitolato speciale di appalto, parte seconda, opere civili - Technical
517 specification for contractors, Part II, Civil Works, Autostrade per l'Italia SpA, Rome, Italy, 2008.

518 [50] Anas, Capitolato Speciale d'Appalto per lavori stradali. Norme tecniche (Standard
519 requirements for road construction. Technical Specifications) (2009).

- 520 [51] VSS, SN 640431 – 1aNA Enrobés bitumineux compactés - Conception, exécution, exigences
521 pour les couches en place Association suisse des professionnels de la route et des transports (VSS),
522 Winterthur, Switzerland, 2003.
- 523 [52] C. Plati, P. Georgiou, A. Loizos, Influence of different roller compaction modes on asphalt mix
524 performance, *International Journal of Pavement Engineering* 17(1) (2016) 64-70.
- 525 [53] G. Flintsch, E. de León, K. McGhee, I. AI-Qadi, Pavement surface macrotexture measurement
526 and applications, *Transportation Research Record: Journal of the Transportation Research Board*
527 (1860) (2003) 168-177.
- 528 [54] F.G. Praticò, A. Astolfi, A new and simplified approach to assess the pavement surface micro-
529 and macrotexture, *Construction and Building Materials* 148(Supplement C) (2017) 476-483.

530

531